PROCEEDINGS OF SPIE

On the use of a liquid lens for improving iris images quality in a hyperspectral system

Ettore Masetti, Luigi Rovati

On The Use of a Liquid Lens for Improving Iris images quality in a Hyperspectral system

Ettore Masetti[a] and Luigi Rovati[a]

[a]Department of Engineering "Enzo Ferrari", University of Modena and Reggio Emilia, Modena, Italy.

ABSTRACT

In this paper, we describe how using a liquid lens can improve the quality of iris images acquired by a hyperspectral system. This improvement in the image quality is especially noticeable for systems that scan the iris over a wide range of wavelengths, e.g. visible and near-infrared spectrum. We have tested this approach on the previously developed system able to acquire iris images in the spectral range 480 - 900 nm. The key novelty presented in this paper is represented by the possibility of adaptively adjusting the focus of the imaging system, allowing for chromatic aberration compensation and ensuring a constant image sharpness among all wavelengths. A fast-tunable liquid lens has been placed in front of the chromatically corrected camera objective to adaptively change the overall focus of the imaging system. The findings imply that the device can rapidly perform hyperspectral measurements of the iris over a broad wavelength range ensuring optimal focus for all images.

Keywords: Liquid lens, hyperspectral imaging, chromatic correction, autofocus.

1. INTRODUCTION

Biomedical optical imaging has made significant advancements that allow for in-depth analysis at tissue microstructure. Hyperspectral imaging is a highly promising technique that combines spectroscopy with imaging to create a non-invasive way to identify and monitor changes in the optical properties of tissue related to various diseases and pathologies. In our previous articles,[1,2] we described the development of a hyperspectral imaging system designed to analyze the spectral reflectance of the human iris. This system provides much more detailed information about the iris's morphology and spectral characteristics compared to traditional colorimetric methods currently used in ophthalmology. By quantitatively measuring the iris's spectral reflectance, we can determine the distribution of key chromophores (such as melanin, hemoglobin, and carotenoids) in the iridal layers and track any changes over time.[3–7]

In this paper, we present the improvements to the experimental setup of our hyperspectral imaging system by introducing an autofocusing configuration using a fast-tunable liquid lens to correct for chromatic aberrations caused by the imaging system's objective lens. Chromatic correction is especially important when using a broadband light source, e.g. from the visible to the near-infrared.

In Section 2, we discuss the paper motivation and present the overall experimental setup with a particular focus on the improvements of the acquisition optics. In Section 3, we describe the calibration method used for chromatic correction and the system implementation to obtain real-time focus correction for each specific illumination wavelength. In Section 4, we report the experimental results, highlighting the improvements in terms of images quality and reflectance measurements derived from chromatic-corrected and non-corrected acquisitions.

Further author information: (Send correspondence to E.M.)
E.M.: E-mail: ettore.masetti@unimore.it, Telephone: +39 059 205 6109

2. MOTIVATION AND MEASURING SYSTEM DESIGN

Chromatic aberration can be a detrimental issue in hyperspectral imaging. It can cause color fringing or distortion in the spectral signature, which can degrade the accuracy and precision of the acquired information. High-quality optics and accurate design are commonly used to minimize this effect. Optimized lenses with low chromatic dispersion can be particularly effective at reducing chromatic aberration in the visible range but are often not very effective if the system also considers near infrared radiation.

Among several active focusing systems, a possible solution is represented by liquid optical lenses with electrically controllable focal lengths. Liquid lenses offer a number of advantages compared to traditional focusing systems that use glass lenses and motors for focus adjustment. These advantages include reduced complexity, size, weight, and power consumption. In ophthalmic instrumentation, another feature of these devices is extremely important. Since the measurement must be performed quickly to avoid discomfort for the patient, the focus adjustment speed is a characteristic of primary importance. Liquid lenses offer, from this point of view, superlative performance compared to other approaches.[5, 8–10]

As a result, a fast-tunable liquid lens has been integrated into the hyperspectral imaging system previously presented by our group.[11] In the following section, the overall design of the hyperspectral system will be described, with a particularly detailed description of the modifications made to the camera optics to integrate the liquid lens.

2.1 Experimental Setup

The hyperspectral imaging system depicted in Figure 1 is composed of three main blocks: the illumination unit, the imaging unit, and the control and data acquisition unit.
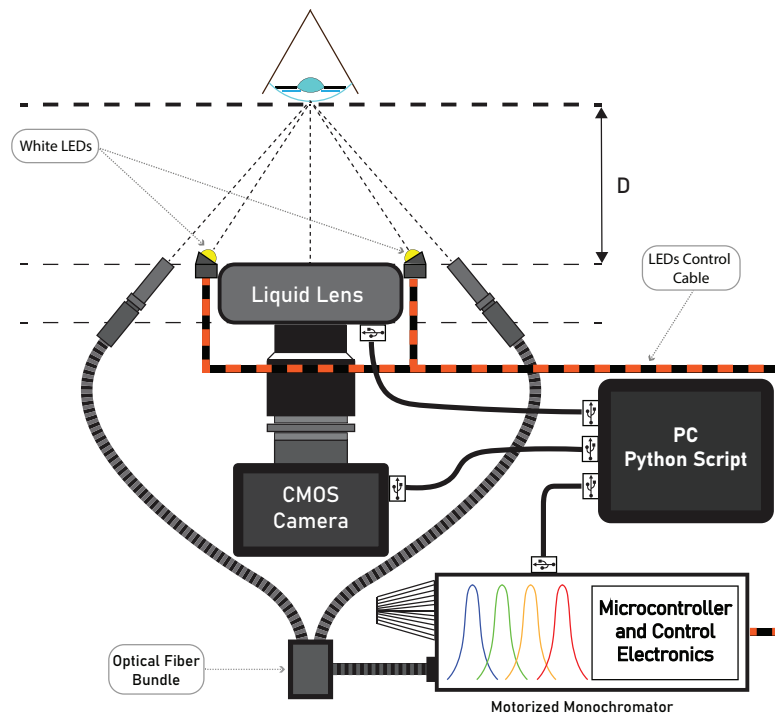

Figure 1: Schematic representation of the hyperspectral imaging system including the liquid optical lens.

Quasi-monochromatic light used to illuminate the patient's iris is generated by a custom monochromator that has been designed to produce a spectral output ranging from 480 to 900 nm, monochromator output spectrum presents a $FWHM = 20$ nm. The monochromator is equipped with a DC motor that rotates the diffraction grating to sweep through the desired wavelengths. A fiber optic bundle is used to direct the monochromator's output light to the iris. Additionally, the light from two white light-emitting diodes (LEDs) is used to aid

in aligning the patient's eye with the hyperspectral imaging (HSI) system and to maintain a constant pupil contraction during HS measurements. Our illumination and imaging system has been designed to position the first Purkinje image within the fully constricted pupil. This maximizes the iris area by causing pupil contraction through the use of white ancillary LEDs and eliminates the need to remove reflections or glare from the region of interest (ROI), which is the iris, during image processing. The aforementioned condition is ultimately obtained when the light sources surface is placed at a distance $D = 50$ mm from the cornea vertex.

The light scattered back by the iris is collected by a C-mount lens (Xenoplan 23 mm, f/1.4, Schneider Kreuznach GmbH, Germany) and captured by a monochrome camera synchronized with the scanning mechanism of the illumination unit. The camera is equipped with a CMOS sensor (GS3-U3-32S4M-C, FLIR Systems, Inc., USA) that is sensitive to both visible and near-infrared radiation. The acquisition system is integrated with a tunable liquid lens (EL-16-40-TC-VIS-5D-M30.5, OptoTune AG, Switzerland) placed on the objective filter mount, for compensating chromatic aberrations introduced by the camera objective lens. The distance between the camera and the iris is 50mm, and the field of view is 20mm x 15mm. A single image is taken at each monochromator wavelength to create the hyperspectral cube. The spatial resolution in the focal plane is 11 μm. The entire set of hyperspectral images is acquired over a period of 8350 ms, with an exposure time of 100ms for each image.

The control unit for the instrument consists of a microcontroller (Arduino Uno, Arduino, Italy) that is connected to a personal computer (PC) running a Python Script. A specialized software program has been developed to manage the instrument and provide a user interface. The control unit synchronizes the image acquisition with scanning the illumination wavelengths and controls the auxiliary and fixation LEDs. The acquired images are saved in designated folders for later analysis.

3. CALIBRATION AND CHARACTERIZATION

3.1 Chromatic Correction Calibration

One fundamental step in performing chromatic correction using a liquid lens is to calibrate the optical system. This procedure allows us to determine the correct electrical polarization to be applied to the liquid lens for each wavelength of the hyperspectral system. During measurement, this information enables the adaptation of the liquid lens's optical power to compensate for any chromatic aberrations introduced by the imaging system. To perform the system calibration, we used a commercial 36 Sectors Siemens target printed on White Photographic Paper (Star Target, by Edmund Optics). The system calibration procedure can be summarized in the following steps:

1. **Manual focus adjustment:** The monochromator is set to generate an initial wavelength of $\lambda_0 = 480$ nm, and the imaging system is manually positioned at a distance from the target to achieve a condition close to the focus.

2. **Optical power liquid lens sweep:** At a defined illumination wavelength λ_k, the liquid lens is set to perform a sweep in optical power in the range of $OP_{range} = (OP_{min}, OP_{max}) = (-0.5 \, \text{D}, 0.5 \, \text{D})$ with a resolution of $\Delta OP = 0.01$ D. The Python script triggers the camera and acquires 1824x1366 px images for each applied correction optical power OP_h: $I_{\lambda_k}(OP_h)$.

3. **Focus optimization:** A Laplacian-based focus metric is applied to all acquired images, $I_{\lambda_k}(OP_h)$, using the Laplacian operator on a 2-dimensional greyscale image, represented as a bidimensional distribution of intensity $I(x, y)$:

$$\nabla \cdot \nabla I = \nabla^2 I = \frac{\partial^2 I}{\partial x^2} + \frac{\partial^2 I}{\partial y^2}. \tag{1}$$

In other words, the Laplacian of the image is defined as the sum of the second partial derivatives. The Laplacian operator highlights regions of an image that have rapid intensity changes, which makes it an effective edge detector. Sharp edges are present only in focused images, while non-sharp features are present in all images. Therefore, an image with high variance of the Laplacian operator over the image has a wider

distribution of sharp and non-sharp features, which indicates a higher degree of focus. Conversely, an image with low variance has a reduced spread of feature sharpness, which corresponds to a negligible amount of sharp edges in the image, i.e. a defocused image. Therefore, the variance of the Laplacian of an image can be used as a metric to quantify the degree of focus and can be computed as:

$$\phi_{i,j} = \frac{1}{\#\Omega(x,y)} \sum_{(i,j)\in\Omega(x,y)} \left(\nabla^2 I(i,j) - \overline{\nabla^2 I} \right)^2,$$ (2)

where $\Omega(x,y)$ is defined as every pixel neighborhood, $\overline{\nabla^2 I}$ is the average value of the image Laplacian over $\Omega(x,y)$ and $\#\Omega(x,y)$ is the cardinality of $\Omega(x,y)$.

Therefore, by calculating the maximum Laplacian variance $\phi_{\lambda_k}(OP_h)|max$, it is possible to determine the optimal optical power $OP\lambda_k$ to achieve the highest image sharpness at a specific illumination wavelength λ_k.

4. **Repeat OP sweep and focus optimization for all wavelengths:** Steps 2 and 3 are repeated for the overall wavelength range $WL_{range} = (480\,\text{nm}, 900\,\text{nm})$ with a wavelength step $\Delta WL = 20\,\text{nm}$. As a result, it is possible to obtain the optimal optical power OP_{λ_k} for each illumination wavelength λ_k.

5. **Repeated measurements:** Steps 1, 2, 3, and 4 are repeated multiple times to improve measurement accuracy. By taking $N = 10$ sets of measurements, we obtain a set $OP_{\lambda_k}|n, 0 < n < N-1$ of optimal optical power for each illumination wavelength λ_k. In step 1, an operator is required to position the imaging system for obtaining the optimal focus at the starting wavelength λ_0. Therefore, it is necessary to correctly combine all the measurements and provide an overall optical power correction $\overline{OP\lambda_k}$ referred to the initial wavelength λ_0. For each wavelength λ_k, the following average operation is performed:

$$\overline{OP_{\lambda_k}} = \frac{1}{N} \sum_{0<n<N} \left(OP_{\lambda_k}|n - OP_{\lambda_0}|n \right),$$ (3)

where $OP_{\lambda_0}|n$ is the optical power correction at the starting wavelength λ_0 referred to the n measurement.
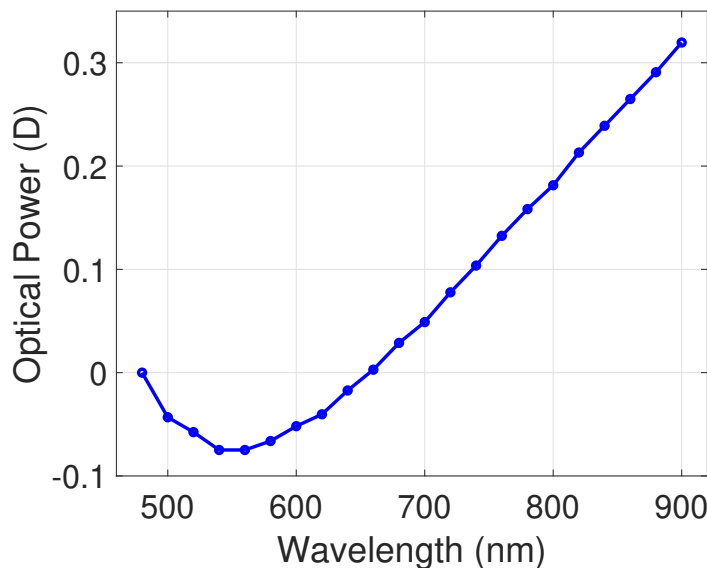

Figure 2: Optical Power calibration curve for chromatic correction of the hyperspectral imaging system.

The described method enables the extraction of the chromatic correction calibration curve as shown in Fig. 2.

3.2 Hyperspectral Chromatic Corrected Measurements

As a result, the hyperspectral system integrated with the liquid lens ensures the maximization of image sharpness for all illumination wavelengths. Once the initial focusing condition is established by the operator, no further computational time is required during the remaining measurement phase as the chromatic calibration curve is directly applied to the initial focusing condition, as represented by the equation:

$$OP_k = OP_0 + \overline{OP_{\lambda_k}}, \tag{4}$$

ensuring an acceptable measurement time for ophthalmic applications.

4. EXPERIMENTAL RESULTS

4.1 Focus Level Evaluation of Corrected Hyperspectral Images of a Reference Siemens Target

As mentioned in Section 3.1, a valid focus metric consists in computing the variance of the Laplacian of the image. Therefore, in order to assess the efficacy of the applied correction curve, it is useful to compare corrected and non-corrected hyperspectral images in terms of Laplacian variance.

The measurement procedure consists of the standard hyperspectral scan from 480 nm to 900 nm, where for each wavelength both corrected and non-corrected images are acquired.

For a proper comparison between images acquired at different focus conditions, it is useful to convert each image corresponding to a specific wavelength into a reflectance map. The conversion is performed using the following equation:

$$R_{i,j}(\lambda_k) = \frac{T_{REF}}{T_{HSI}} \cdot \frac{I_{i,j}(\lambda_k) - D_{i,j}(\lambda_k)}{I_{REF\,i,j}(\lambda_k) - D_{REF\,i,j}(\lambda_k)} \cdot R_{cal\%}. \tag{5}$$

Therefore, the Laplacian Variance operator employed in Section 3.1, is now applied to the hyperspectral reflectance map corresponding to corrected and not corrected images. In other words, the focus metric of a given reflectance map $R_{i,j}$ is computed as:

$$\sigma_{\mathcal{L},R} = \phi_o(\mathcal{L}(R_{i,j})), \tag{6}$$

where $\mathcal{L}$ is the 2D Laplacian operator (Eq. 1) and ϕ_0 is the variance operation extended to the entire image (Eq. 2).
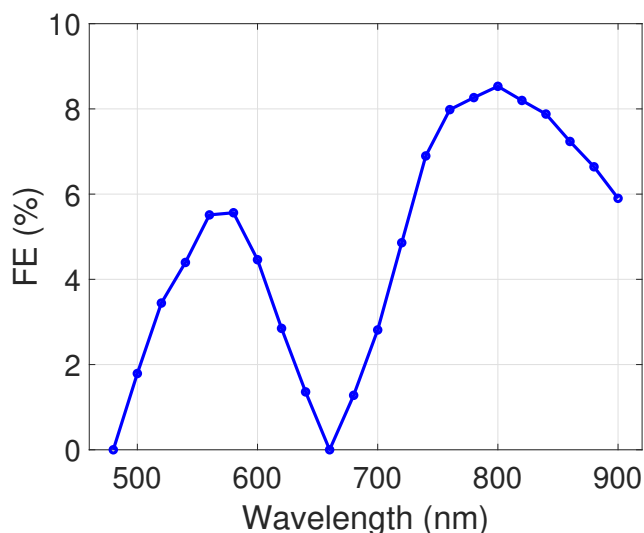

Figure 3: Enhancement Factor (EF) of corrected images acquired using a reference Siemens target.

It is possible to define a Focus Enhancement ($FE_\%$) figure of merit as:

$$FE_\%(\lambda_k) = \frac{\sigma_{\mathcal{L},R-c}(\lambda_k) - \sigma_{\mathcal{L},R-nc}(\lambda_k)}{\sigma_{\mathcal{L},R-c}(\lambda_k)} \cdot 100, \tag{7}$$

where the subscripts c and nc refer to corrected and non-corrected images respectively.

Fig. 3 shows $FE_\%$ as a function of the illumination wavelength λ_k. The results indicate a positive correlation between the magnitude of the correction factor and the improvement in focus. Specifically, as the absolute value of the correction factor increases, the improvement in focus also increases. Conversely, when the correction factor is null, no statistically significant change in focus is observed.

4.2 Qualitative Focus Improvement Evaluation and Average Reflectance Results of Corrected Hyperspectral Images of the Human Iris

In this preliminary stage of the study, the proposed focus evaluation algorithm is not precise enough to quantitatively determine the focus enhancement in a complex target as the human iris. Therefore, we represent corrected and non-corrected images side-by-side at different wavelengths in Fig. 4.

A) 560 nm
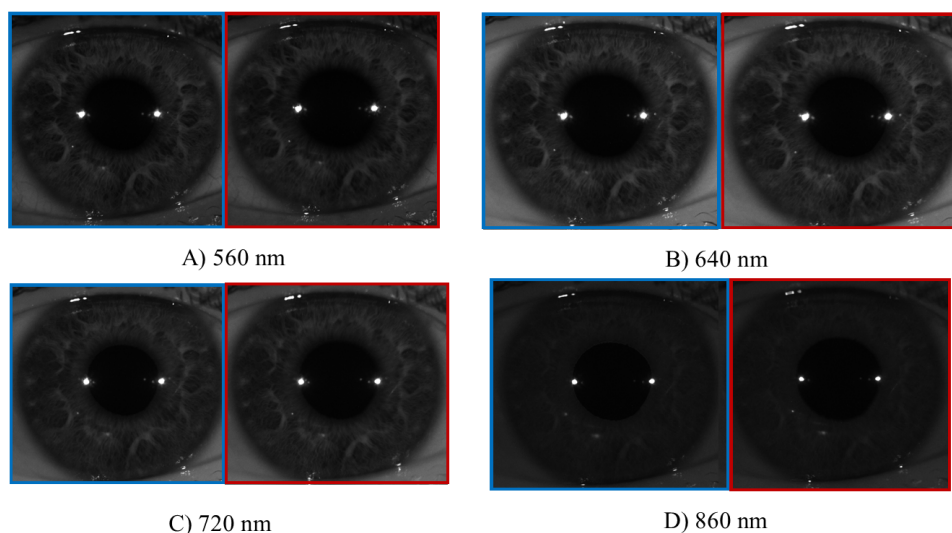
B) 640 nm

C) 720 nm

D) 860 nm

Figure 4: Hyperspectral images at specific wavelengths, comparison between corrected (blue labeled) and non-corrected (red labeled) images.

These images provide a visual aid of how the chromatic correction enhances the focus quality of the images in the overall wavelength range.

5. CONCLUSIONS

In conclusion, this study demonstrates the efficacy of incorporating a fast-tunable liquid lens into a hyperspectral imaging system for the acquisition of iris images. By adaptively adjusting the focus of the imaging system and compensating for chromatic aberration, the liquid lens significantly improves image quality across a wide range of wavelengths, specifically in the visible and near-infrared spectrum. The results of this study indicate that the use of a liquid lens in hyperspectral iris imaging improves overall image sharpness and allows for rapid, high-quality measurements of the iris over a broad wavelength range.

REFERENCES

[1] Di Cecilia, L., Marazzi, F., Rovati, L., and Rovati, L., "Hyperspectral imaging of the human iris," *Optica Publishing Group* , 104120R (June 2017).

[2] Di Cecilia, L. and Rovati, L., "Design and performance of a hyperspectral imaging system: Preliminary in vivo spectral reflectance measurements of the human iris," *Rev. Sci. Instrum.* **91**, 014104 (Jan. 2020).

[3] Boyce, C., Ross, A., Monaco, M., Hornak, L., and Li, X., "Multispectral Iris Analysis: A Preliminary Study51," in [*2006 Conference on Computer Vision and Pattern Recognition Workshop (CVPRW'06)*], 51, IEEE (June 2006).

[4] Vilaseca, M., Mercadal, R., Pujol, J., Arjona, M., de Lasarte, M., Huertas, R., Melgosa, M., and Imai, F. H., "Characterization of the human iris spectral reflectance with a multispectral imaging system," *Appl. Opt.* **47**, 5622–5630 (Oct. 2008).

[5] Medina, J. M., Pereira, L. M., Correia, H. T., and Nascimento, S. M., "Hyperspectral optical imaging of human iris in vivo: characteristics of reflectance spectra," in [*Journal of Biomedical Optics, Vol. 16, Issue 7*], **16**, 076001, SPIE (July 2011).

[6] Di Cecilia, L., Marazzi, F., and Rovati, L., [*A hyperspectral imaging system for the evaluation of the human iris spectral reflectance*], vol. 10045 (Feb. 2017).

[7] di Cecilia, L. and Rovati, L., "Performance analysis of a hyperspectral system for human iris imaging," in [*Proceedings Volume 10858, Ophthalmic Technologies XXIX*], **10858**, 88–95, SPIE (Feb. 2019).

[8] "Vision-R 700 Auto Phoropter."

[9] Amirsolaimani, B., Peyman, G., Schwiegerling, J., Bablumyan, A., and Peyghambarian, N., "A new low-cost, compact, auto-phoropter for refractive assessment in developing countries," *Scientific Reports* **7**, 13990 (Oct. 2017).

[10] Menolotto, M., Livingstone, I. A. T., and Giardini, M. E., "An Imaging-based Autorefractor," in [*2021 IEEE International Instrumentation and Measurement Technology Conference (I2MTC)*], 1–6 (May 2021). ISSN: 2642-2077.

[11] Di Cecilia, L., Marazzi, F., and Rovati, L., "An improved imaging system for hyperspectral analysis of the human iris," in [*2017 IEEE 3rd International Forum on Research and Technologies for Society and Industry (RTSI)*], 1–5, IEEE (Sept. 2017).